Mon. Not. R. Astron. Soc. **000**, 1–?? (2003) Printed 8 October 2018 (MN LaTeX style file v2.2)

Galactic distribution of merging neutron stars and black holes – prospects for short γ-ray burst progenitors and LIGO/VIRGO

R. Voss⋆ and T. M. Tauris⋆
Astronomical Observatory, Niels Bohr Institute, University of Copenhagen, DK-2100 Copenhagen Ø, Denmark

Received 2002 December 5; Accepted 2003 March 11

ABSTRACT
We have performed detailed population synthesis on a large number (2×10^7) of binary systems in order to investigate the properties of massive double degenerate binaries. We have included new important results in our input physics in order to obtain more reliable estimates of the merging timescales and relative formation rates. These improvements include refined treatment of the binding energy in a common envelope, helium star evolution and reduced kicks imparted to newborn black holes. The discovery and observations of GRB afterglows and the identification of host galaxies have allowed comparisons of theoretical distributions of merger sites with the observed distribution of afterglow positions relative to host galaxies. To help investigate the physical nature of short- and long-duration γ-ray bursts (GRBs), we compute the distances of merging neutron stars (NS) and/or black holes (BH) from the centers of their host galaxies, as predicted by their formation scenario combined with motion in galactic potentials. Furthermore, we estimate the formation rate and merging rate of these massive double degenerate binaries. The latter is very important for the prospects of detecting gravitational waves with LIGO/VIRGO. We find that the expected detection rate for LIGO II is ~ 850 yr^{-1} for galactic field sources and that this rate is completely dominated by merging BHBH binaries. Even LIGO I may detect such an event (~ 0.25 yr^{-1}). Our preferred model estimate the Galactic field NSNS merger rate to be $\sim 1.5 \times 10^{-6}$ yr^{-1}. For BHBH systems this model predicts a merger rate of $\sim 9.7 \times 10^{-6}$ yr^{-1}. Our studies also reveal an accumulating numerous population of very wide orbit BHBH systems which never merge ($\tau \gg \tau_{\rm Hubble}$).

Key words: methods: numerical – binaries: close – gravitational waves – stars: formation – neutron stars – black holes – gamma-rays: bursts

1 INTRODUCTION

It has been recognized for a long time that the time duration of GRBs is bimodal: the majority (75%) of the bursts have a long duration with a mean of $\sim$ 20 sec., the rest have a much shorter duration with a mean of only $\sim$ 0.2 sec. (Mazets et al. 1981 and Hurley et al. 1992). Both of these two classes of GRBs have similar isotropic spatial distributions, but differ with respect to spectral hardness, fluence and temporal pulse properties (e.g. Kouveliotou et al. 1993; Lee & Petrosian 1997 and Norris et al. 2000). It is natural to suggest that two distinct types of progenitors are responsible for the existence of the two observed distinct populations of GRBs.

Since it has been established from measurements of GRB redshifts that their distance scales are cosmological (Metzger et al. 1997), GRB scenarios require an energy release output of roughly $(\Omega_\gamma/4\pi) \times 10^{54}$ erg, where Ω_γ is the beaming angle. According to the internal shock model for the production of the observed γ-rays (e.g. Piran 2000, and references therein), the duration of a burst is very likely to be a direct measure of the time interval during which the powering engine is active. In both of the main scenarios the basic ingredient is a black hole surrounded by an accretion disk of nuclear matter threaded by a strong magnetic field. A large disk viscosity causes the matter to spiral inwards on a timescale of minutes. The poloidal part of the magnetic field in the inner disk, spinning at millisecond periods, will then accelerate a small amount of material (less than $10^{-5}\ M_\odot$) in the form of a narrow and highly relativistic jet (this is the so-called Blandford-Znajek mechanism, e.g. Lee, Wijers & Brown 2000). Alternatively, the jet of material is produced by annihilating neutrinos along the disk axis. These neutrinos result from the release of binding energy of the rapidly accreted ($> 0.01\ M_\odot$) material. In either mechanism, the relativistic jet becomes a fireball and ultimately produces the GRB.

The most promising models to account for the long and short duration bursts involve the collapse of a massive star (e.g. Woosley 1993 and MacFadyen & Woosley 1999) and the merging of compact objects caused by the in-spiral due to gravitational wave emission in a tight binary (e.g. Goodman 1986; Eichler et al. 1989; Paczyński 1990 and Meszaros & Rees 1992), respectively. These associations are supported by simulations of outburst dura-

⋆ E-mail: voss@astro.ku.dk (RV); tauris@astro.ku.dk (TMT)

tions which are estimated to be ∼several tens of seconds for the relativistic outflow generated by the collapse of a massive star (MacFadyen & Woosley 1999), and < 1 sec (Lee & Kluzniak 1998; Ruffert & Janka 1999) for the neutrino-driven wind of merging compact objects, respectively. It has been demonstrated (Meszaros, Rees & Wijers 1998) that both models are able to produce the required GRB energies.

An important method to test the above scenarios is by determining the locations and environments in which the GRBs must occur according to their respective models. Collapsars (collapsing massive stars) are expected to be found close to their place of birth as a result of the short lifetime (a few Myr) of their progenitors. Therefore, these GRBs should occur in dense, dusty star-forming regions – i.e. inside their host galaxies. This hypothesis is in agreement with the observations of long-duration GRB afterglows: there seems to be a correlation between GRB locations and the UV light of their host galaxies (Sahu et al. 1997; Fruchter et al. 1998; Kulkarni et al. 1998, 1999; Bloom, Kulkarni & Djorgovski 2002). Furthermore, an underlying supernova component (a "bump") seems to be present in the light curves of GRB 980326 (Bloom et al. 1999) and GRB 970228 (Reichart 1999; Galama et al. 2000), and recent detections of an iron line in the afterglow of several GRBs also provides evidence for the presence of a dense matter in the vicinity of the bursts (e.g. Yoshida et al. 1999; Piro et al. 1999, 2000; Vietri et al. 1999).

All of the above mentioned afterglow observations only originate from long-duration GRBs. So far, no similar types of observations have been possible for the short bursts. It is the hope that observations of the short bursts will be possible in the near future. An analysis of the expected afterglow properties of these bursts is, for example, given by Perna & Belczynski (2002), while the prospect of future observations of these afterglows are discussed by Panaitescu, Kumar & Narayan (2001). The main topic to be investigated is the distribution of merging compact binaries with respect to their host galaxies. The reason is that the two supernova explosions in the progenitor binaries result in systemic recoil velocities of typically a few hundred km s^{-1}, and therefore the merging compact binaries have the potential to travel far from their birth places – if their merger timescale is relatively large. However, the latter issue depends on the final orbital separation of the binaries, after the second star collapses to form a supernova.

To estimate the merger timescales (and thus the offset of the associated GRBs from their birth places) it is necessary to perform a binary population synthesis study of their progenitors. Such studies have been performed recently in a number of papers: e.g. Bloom, Sigurdsson & Pols (1999); Belczynski, Kalogera and Bulik (2002); Perna & Belczynski (2002); Belczynski, Bulik and Kalogera (2002); Sipior & Sigurdsson (2002). The applied formation scenarios, input physics and subsequent results of these studies are not conclusive. Our major concern, however, is that all of the above papers have assumed rather simplified calculations e.g. for the very important common envelope and spiral-in phase by using a constant value for the so-called λ-parameter.

Here we use Monte Carlo simulations to determine the range of potential runaway velocities, orbital separations and merger timescales as predicted by the standard model for the formation of neutron star/black hole binaries. We include the many recent developments in the field which severely affects the input physics and the outcome – especially the helium star evolution and the binding energy during the common envelope evolution. Also the question of kicks imparted to newborn black holes has been revisited after the recent detection of the space velocity of the black hole binary GRO J1655–40 (Mirabel et al. 2002). Our binaries are launched into galaxies with various masses. Initially the binaries are placed in starforming regions and we keep track of their motion caused by recoil impacts from the supernova explosions of the stellar components. The resulting merger site distributions of the compact binaries are then explored for the different galactic potentials.

Population synthesis of massive binaries is also an important tool to constrain the local merging rate of NS/BH-binaries in order to predict the number of events detected by the gravitational wave observatories LIGO/VIRGO. As a compact binary continue its inspiral, the gravitational waves sweep upward in frequency from about 10 Hz to 10^3 Hz, at which point the compact stars will collide and coalesce. It is the last 15 minutes of inspiral, with ∼ 16 000 cycles of waveform oscillation, and the final coalescence, that LIGO/VIRGO seeks to monitor. LIGO I and LIGO II (the advanced interferometer) are expected to detect NSNS inspiral events out to a distance of ∼ 20 Mpc and ∼ 300 Mpc, respectively, according to recent estimates (Thorne 2001). However, as a result of their larger chirp masses, merging double black hole binaries (BHBH) are detected out to a distance which is ∼5 times larger (see e.g. Sipior & Sigurdsson 2002). We have therefore extended our work to also include these systems.

It is the hope that future observations will reveal a combined gravitational wave and GRB source. This should be possible given the angular resolution of ∼1 degree on the sky from simultaneous detections using both LIGO and VIRGO. To establish such a connection between these two events would reveal interesting new insight to the physics involved. Also by comparing the arrival times of the gravitational waves and the earliest gamma rays, it should be possible to measure the relative propagation speeds of light and gravitational waves to an accuracy ∼ 10^{-17} (Thorne 2001).

In our binary notation we distinguish between BHNS, where the black hole is formed *before* the neutron star, and NSBH where the black hole is formed *after* the neutron star. NSNS and BHBH refer to double neutron star and double black hole systems, respectively. In Section 2 we describe our model for making neutron star/black hole binaries via interacting binary evolution. Our modelling of galactic potentials and binary star formation rates are presented in Section 3. In Section 4 we summarize our results and in Section 5 we follow up with discussions and compare with previous work. Finally, our conclusions are given in Section 6.

2 FORMATION OF NEUTRON STAR/BLACK HOLE BINARIES

In Fig. 1 we have shown the standard evolutionary sequences leading to the formation of a double neutron star system. The (recycled) neutron stars are detected as radio pulsars. The scenario for producing a black hole/neutron star binary system is similar. As can be seen from the figure the progenitor systems evolve through a high-mass X-ray binary (HMXB) phase. The formation of a HMXB requires two relatively massive stars (> 12 $M_\odot$) on the ZAMS. Alternatively, the secondary star can be less massive initially, as long as it gains enough material from the primary star so that it will later end up above the threshold mass for undergoing a supernova explosion (like the primary star). The first mass transfer phase, from the primary to the secondary star, is usually assumed to be dynamically stable (semi-conservative) since the mass ratio, at the onset of the RLO, is not too extreme. However later on, when the secondary star evolves, *all* HMXBs must end up in a common envelope phase, as the neutron star (or low-mass black hole) is engulfed by the

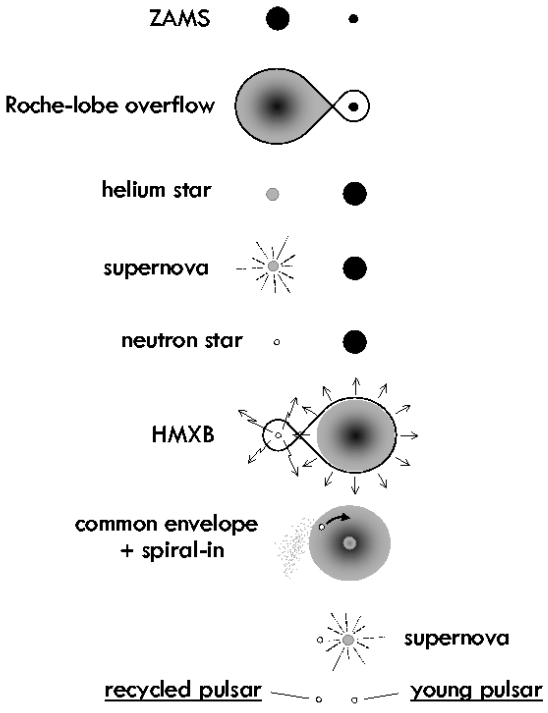

Figure 1. Cartoon depicting the formation of a HMXB and finally a double neutron star (and/or black hole binary system). Such a binary will experience two supernova explosions. It is always the recycled pulsar which is observed in a double pulsar system as a result of its very long spin-down timescale compared to a young pulsar (a factor of $\sim 10^2$). If the final system is very tight it will coalesce as a result of gravitational wave radiation.

extended envelope of its companion, in an orbit which is rapidly shrinking due to significant loss of orbital angular momentum. This stage of binary evolution is extremely important, since the outcome is a huge reduction of the orbital separation or merging of the stellar components – see Sect. 2.4. Stellar winds of massive stars, as well as of naked helium cores (Wolf-Rayet stars), are also some of the most uncertain aspects of the modelling of HMXB evolution. Finally, the physical conditions which determine the formation of a neutron star versus a black hole are also still quite unknown. Below we shall briefly outline our model of binary evolution.

2.1 Stellar evolution models

We used Eggletons numerical stellar evolution code to collect a large array of grid points for stars with masses in the interval $0.9 - 100\,M_\odot$. This code uses a self-adaptive, non-Lagrangian mesh-spacing which is a function of local pressure, temperature, Lagrangian mass and radius. It treats both convective and semi-convective mixing as a diffusion process and finds a simultaneous and implicit solution of both the stellar structure equations and the diffusion equations for the chemical composition. New improvements are the inclusion of pressure ionization and Coulomb interactions in the equation-of-state, and the incorporation of recent opacity tables, nuclear reaction rates and neutrino loss rates. The most important recent updates of this code are described in Pols et al. (1995, 1998) and some are explained in Han et al. (1994). In our standard model we used a chemical composition of (X=0.70, Z=0.02) and assumed a mixing-length parameter of

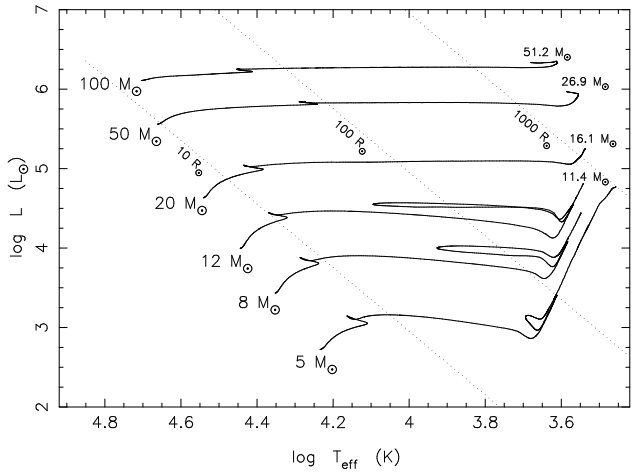

Figure 2. Evolutionary tracks for a few selected stars in our code (X=0.70, Z=0.02). For the massive stars ($12 - 100\,M_\odot$) the final mass, after stellar wind mass loss, is written at the end of the tracks.

$\alpha = l/H_p = 2.0$. The uncertainty of these values (and their temporal evolution) is not very significant for the results of our work in consideration here, given the many major uncertainties of parameters governing the mass-transfer phases, spiral-in, helium star wind, supernova explosion etc. Convective overshooting is taken into account in the same way as in Pols et al. (1998) using an overshooting constant $\delta_{\rm ov} = 0.10$. We used de Jager's work (de Jager et al. 1988; Nieuwenhuijzen & de Jager 1990) to estimate the wind mass loss prior to the mass-transfer phase. Examples of our stellar evolutionary tracks are shown in Fig. 2. We calculated $\sim 40\,000$ grid points of fine mesh spacing in the HR-diagram in order to perform fast Monte Carlo population synthesis.

2.2 A model of binary evolution

In general terms our model follows the standard model for the formation and evolution of HMXBs. Therefore, in the following we shall mainly discuss the issues below where our model applies different input physics compared to earlier work. For a general discussion of close binary evolution we refer to, for example, van den Heuvel (1994) and Tauris & van den Heuvel (2003).

To simulate the formation of massive double degenerate binaries we assume that the initial binary system consists of two zero-age main sequence (ZAMS) stars, and chose primary masses in the interval $10 - 100\,M_\odot$ using a Salpeter-like IMF, $N(m) \propto m^{-2.70}$ (Scalo 1986). The secondary stars (less massive than their primary companions) were chosen in the interval $4 - 100\,M_\odot$ according to the mass-ratio function: $f(q) = 2/(1+q)^2$ (Kuiper 1935). We adopt the term "primary" to refer to the *initially* more massive star, regardless of the effects of mass transfer or loss as the system evolves. The initial orbital separations were chosen between $5 - 10\,000\,R_\odot$ from a distribution flat in $\log a$.

2.3 Helium stars, SN kicks and remnant masses

For low-mass stars, the mass of the helium core in post main-sequence evolution is practically independent of the presence of an extended hydrogen-rich envelope. However, for more massive stars

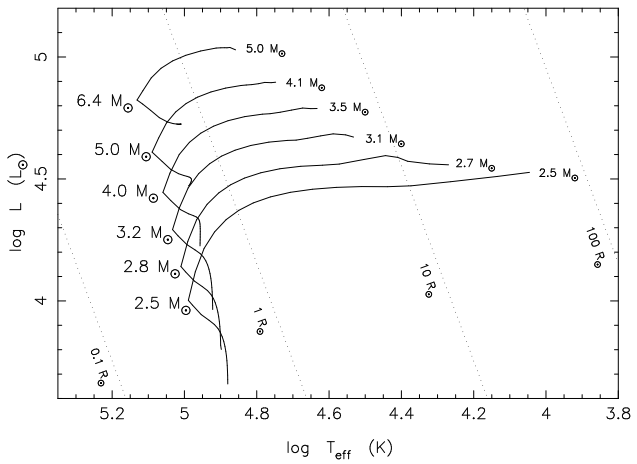

Figure 3. Evolutionary tracks for selected helium stars in our code (Y=0.98, Z=0.02). The final mass (after stellar wind mass-loss) is written at the end of the tracks. The expansion of these (low-mass) helium stars in close binaries often results in a secondary mass-transfer phase. The more massive Wolf-Rayet stars do not expand very much during their evolution. Almost all the He is burned into C, O and subsequently Ne. After O. Pols (priv. comm.)

($> 2\,M_\odot$) the evolution of the core of an isolated star differs from that of a naked helium star (i.e. a star which has lost its hydrogen envelope via mass transfer in a close binary system). It is very important to incorporate the giant phases of helium star evolution. Of particular interest are the low-mass helium stars ($M_{\rm He} < 3.5\,M_\odot$) since they swell up to large radii during their late evolution (e.g. Habets 1986). This may cause an additional phase of mass transfer from the naked helium star to its companion (often referred to as case BB mass transfer). Recent detailed studies of helium stars in close binaries have been performed by Dewi et al. (2002), Dewi & Pols (2003) and Ivanova et al. (2003). It should be noticed that helium cores in binaries have tiny envelopes of hydrogen ($< 0.01\,M_\odot$) when they detach from Roche-lobe overflow (RLO) mass transfer. This tiny envelope seems to have important effects on the subsequent radial evolution of the helium star (e.g. Han et al. 2002).

The evolution of more massive helium stars (Wolf-Rayet stars) is also quite important. There is currently not a clear agreement on the rate of intense wind mass-loss from Wolf-Rayet stars (e.g. Wellstein & Langer 1999; Nugis & Lamers 2000; Nelemans & van den Heuvel 2001). A best estimate fit to the wind mass-loss rate of Wolf-Rayet stars is, for example, given by Dewi et al. (2002). We have adopted their helium star models (Z=0.02, Y=0.98), including wind mass-loss, as calculated by Onno Pols (private communication) – see Fig. 3. The uncertainty in determining the wind mass-loss rate also affects the threshold mass for core collapse leading to a black hole (Schaller et al. 1992; Woosley, Langer & Weaver 1995; Brown, Lee & Bethe 1999). However, it may well be that core mass is not the only important factor to determine the outcome. Magnetic field and spin of the collapsing core could also play a major role (Ergma & van den Heuvel 1998; Fryer & Heger 2000). Furthermore, it seems clear from observations that there is an overlap in the mass range for making a neutron star versus a black hole. In our code we adopted the threshold values given in Table 1. The threshold mass for the CO-core corresponds to a helium star which has experienced another RLO (case BB) in its giant phase and thereby lost its helium envelope.

Table 1. Threshold masses for producing black holes and neutron stars

Remnant	Helium core	CO-core	$M_{\rm ZAMS}^{\rm min}$
Black hole	$5.5\,M_\odot$	$4.0\,M_\odot$	$22 \sim 25\,M_\odot$ *
Neutron star	$2.8\,M_\odot$	$1.7\,M_\odot$	$10 \sim 12\,M_\odot$ *

* Depending on the evolutionary status at the onset of RLO (case C or B).

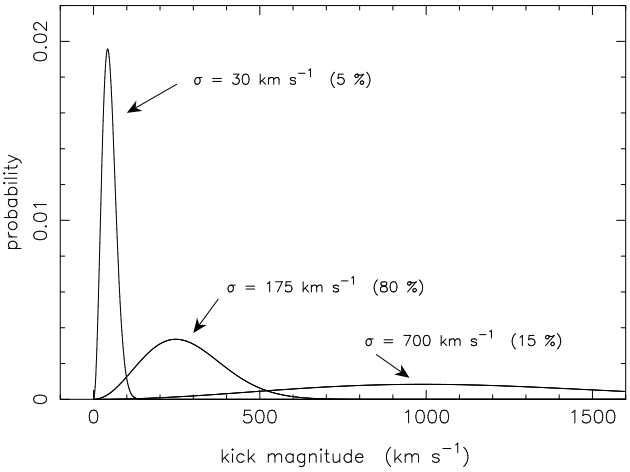

Figure 4. A momentum kick is assumed to be imparted to all newborn neutron stars. The kick magnitude of the asymmetric SN was drawn from a weighted sum of the three Maxwellian distributions shown above. The direction of the kicks is assumed to be isotropic. Black holes were assumed to be accompanied with a smaller kick velocity – see text for description.

We assumed all neutron stars to be formed in asymmetric SNe with a mass of $1.3\,M_\odot$ and chose the 3-D magnitude of the kicks from a weighted sum of three Maxwellian distributions of speeds with $\sigma_w = 30, 175$ and 700 km s^{-1} (5%, 80% and 15%, respectively – see Fig. 4). The choice of this distribution is partly motivated by the study of Cordes & Chernoff (1998), but also includes a low-velocity component to account for the many neutron stars retained in rich globular clusters like 47 Tuc (e.g. Pfahl et al. 2002). Furthermore, we assumed the direction of the kicks to be isotropic (see however Lai, Chernoff & Cordes 2001) and neglected any impact on the companion star from the ejected shell. The recent determination of the run-away velocity (112 ± 18 km s^{-1}) of the black hole binary GRO J1655–40 (Mirabel et al. 2002) seems to suggest that also a stellar collapse leading to the formation of a black hole is accompanied by a momentum kick. In our standard model we apply a reduced kick in the formation process of black holes. We do this by assuming that a similar linear momentum, comparable to that imparted to neutron stars, is given to black holes, such that their resulting kick velocities are reduced by a factor of $M_{\rm BH}/M_{\rm NS}$ with respect to our kick distribution applied on newborn neutron stars. For the masses of the black holes we assumed a mass loss fraction of 30% during the stellar collapse (Nelemans, Tauris & van den Heuvel 1999).

2.4 Common envelope and spiral-in evolution

Except for a few cases in which the two stars in a massive binary are born on the ZAMS with almost equal masses (Brown 1995), the system will evolve through a HMXB-phase and subsequently enter a common envelope and spiral-in phase. In our code we follow the treatment of common envelope evolution introduced by Dewi & Tauris (2000). The same method has been applied recently by others, e.g. Podsiadlowski, Rappaport & Han (2002). Hence, we calculate the binding energy of the stellar envelope by integrating through the outer layers of the donor star:

$$E_{\rm bind} = -\int_{M_{\rm core}}^{M_{\rm donor}} \frac{GM(r)}{r} dm + \alpha_{\rm th} \int_{M_{\rm core}}^{M_{\rm donor}} U dm \quad (1)$$

where the first term is the gravitational binding energy and U is the internal thermodynamic energy (Han et al. 1994, 1995). The value of $\alpha_{\rm th}$ depends on the details of the ejection process, which are very uncertain. A value of $\alpha_{\rm th}$ equal to 0 or 1 corresponds to maximum and minimum envelope binding energy, respectively. By adopting the energy formalism of Webbink (1984) and de Kool (1990), we then equate this envelope binding energy with the release of orbital energy in order to estimate the reduction of the orbit during spiral-in: $E_{\rm bind} \equiv \eta_{\rm CE}\ \Delta E_{\rm orb}$ where $\eta_{\rm CE}$ describes the efficiency of ejecting the envelope, i.e. of converting orbital energy into the kinetic energy that provides the outward motion of the envelope. The total change in orbital energy is then simply given by:

$$\Delta E_{\rm orb} = -\frac{GM_{\rm core}M_1}{2\,a_{\rm f}} + \frac{GM_{\rm donor}M_1}{2\,a_{\rm i}} \quad (2)$$

where $M_{\rm core} = M_{\rm donor} - M_{\rm env}$ is the mass of the helium core of the evolved donor star; M_1 is the mass of the companion star; $a_{\rm i}$ is the initial separation at the onset of the RLO and $a_{\rm f}$ is the final orbital separation after the CE-phase. The orbital separation of the surviving binaries is quite often reduced by a factor of ~ 100 as a result of the spiral-in. If there is not enough orbital energy available to eject the envelope the stellar components will coalesce. For massive stars ($M > 10\,M_\odot$) this method results in so-called λ-values $< 0.1 - 0.01$ (Dewi & Tauris 2001; Podsiadlowski, Rappaport & Han 2002). These values are much smaller than the constant value of $\lambda \sim 0.5$ often used in the literature (e.g. Hurley, Tout & Pols 2002; Sigurdsson & Pols 1999; Fryer, Woosley & Hartmann 1999; Portegies Zwart & Yungelson 1998, or alternatively, $\lambda\,\eta_{\rm CE}$ is used as a single free parameter: Belczynski, Kalogera & Bulik 2002; Belczynski, Bulik & Kalogera 2002; Perna & Belczynski 2002). This result has the very important consequence that in our study many HMXBs will not produce double neutron star/black hole systems because they merge during their subsequent CE-phase (however, those systems that do survive are generally in tight orbits often leading to additional helium star mass transfer and formation of double degenerate systems merging on a short timescale).

It should be noticed that the exact determination of λ depends on how the core boundary is defined (see Tauris & Dewi 2001 for a discussion). For example, if the core boundary (bifurcation point of envelope ejection in a CE) of the 20 $M_\odot$ in Fig.5 is moved out by 0.1 $M_\odot$ then λ is typically increased by a factor of ~ 2.

2.4.1 Helium star common envelope

We take into account that some helium stars, in their giant stages, regain contact with their compact companion star. This leads to a second mass-transfer phase resulting in a naked CO-core, if the stellar components do not coalesce. From detailed helium star analysis, Dewi & Pols (2003) discovered that there is a critical mass

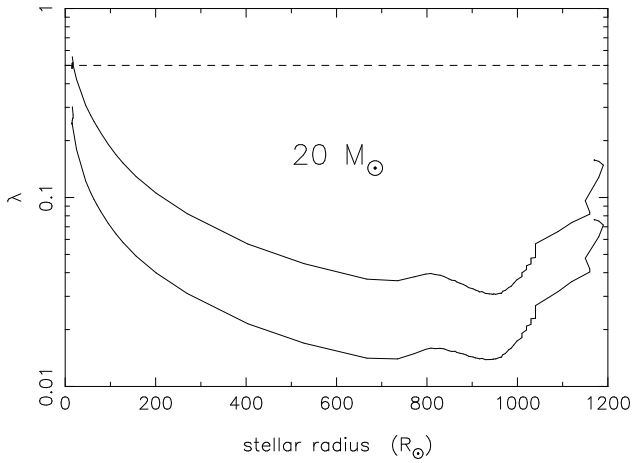

Figure 5. The λ-parameter for a 20 $M_\odot$ star as a function of stellar radius. The upper curve includes internal thermodynamic energy ($\alpha_{\rm th} = 1$) whereas the lower curve is based on the sole gravitational binding energy ($\alpha_{\rm th} = 0$) – see Eq. 1. There is a factor $\sim$2 in difference between the λ-curves in accordance with the virial theorem. It is a common misconception to use a constant (and large) value of $\lambda \simeq 0.5$ marked by the dashed line. In this plot the stellar core is defined as the region where X< 0.10. See text.

($M_{\rm He}^{\rm crit} \sim 3.3\,M_\odot$) above which the RLO from the helium star to a neutron star is dynamically stable. Below this value the system will evolve into a CE and spiral-in phase as a consequence of the rapid expansion of the low-mass helium star. We adopted this value in our code to determine the fate of helium star CE (see however Ivanova et al. 2003 for a different point of view). Typical helium star λ-values are $0.01 - 0.2$ depending on radius and $\alpha_{\rm th}$.

2.4.2 Released accretion energy during CE evolution

Even though the spiral-in timescale is very short (< 1000 yr) for common envelope evolution (Taam & Sandquist 2000), and the accretion rate is limited by the photon radiation pressure (the Eddington limit), the gravitational potential energy release from the $\sim 10^{-5}\,M_\odot$ accreted onto the neutron star or black hole contribute to expel the envelope of the donor star. We modelled this effect by assuming a total energy release of $\Delta E_{\rm acc} \sim \tau_{\rm ce}\,L_{\rm Edd} = 3.8 \times 10^{48}\,(M_{\rm X}/M_\odot)$ erg, and twice this amount for helium star CE, where $M_{\rm X}$ is the mass of the compact object. Given the high column density inside the common envelope a significant part of this energy will be absorbed and facilitate the ejection of the envelope and thereby increase the post-CE orbital separation by a factor:

$$a_{\rm f}^* = a_{\rm f}\,(1 + \Delta E_{\rm acc}/E_{\rm bind}) \quad (3)$$

The average value of this factor is ~ 1.8 for all our systems evolving through a CE-phase (the typical value is only ~ 1.3, but a few systems with very evolved donors have $\Delta E_{\rm acc} > E_{\rm bind}$ and a corresponding correction factor up to about 5).

2.5 RLO and the orbital angular balance equation

The orbital angular momentum of a binary system is given by:

$$J_{\rm orb} = |\vec{r} \times \vec{p}| = \frac{M_1 M_2}{M}\,\Omega\,a^2\,\sqrt{1-e^2} \quad (4)$$

where a is the separation between the stellar components, M_1 and M_2 are the masses of the accretor and donor star, respectively, $M = M_1 + M_2$ and the orbital angular velocity, $\Omega = \sqrt{GM/a^3}$. Here G is the constant of gravity. Tidal effects acting on a near-RLO (giant) star will circularize the orbit on a short timescale of $\sim 10^4$ yr (Verbunt & Phinney 1995) and in the equation below we therefore disregard any small eccentricity ($e = 0$). A simple logarithmic differentiation of the above equation yields the rate of change in orbital separation:

$$\frac{\dot{a}}{a} = 2\,\frac{\dot{J}_{\rm orb}}{J_{\rm orb}} - 2\,\frac{\dot{M}_1}{M_1} - 2\,\frac{\dot{M}_2}{M_2} + \frac{\dot{M}_1 + \dot{M}_2}{M} \tag{5}$$

where the total change in orbital angular momentum is:

$$\frac{\dot{J}_{\rm orb}}{J_{\rm orb}} = \frac{\dot{J}_{\rm gwr}}{J_{\rm orb}} + \frac{\dot{J}_{\rm mb}}{J_{\rm orb}} + \frac{\dot{J}_{\rm ls}}{J_{\rm orb}} + \frac{\dot{J}_{\rm ml}}{J_{\rm orb}} \tag{6}$$

These two equations constitute the orbital angular momentum balance equation. The first term on the right-hand side of this equation gives the change in orbital angular momentum due to gravitational wave radiation (Landau & Lifshitz 1958). The second term in Eq. 6 arises from so-called magnetic braking (this mechanism is not relevant for HMXBs). The third term ($\dot{J}_{\rm ls}/J_{\rm orb}$) on the right-hand side of Eq. (6) describes possible exchange of angular momentum between the orbit and the donor star due to its expansion or contraction (Tauris 2001). Finally, the last term in Eq. (6) represents the change in orbital angular momentum caused by mass loss from the binary system. This is usually the dominant term in the orbital angular momentum balance equation and its total effect is given by:

$$\frac{\dot{J}_{\rm ml}}{J_{\rm orb}} = \frac{\alpha + \beta q^2 + \delta\gamma(1+q)^2}{1+q}\,\frac{\dot{M}_2}{M_2} \tag{7}$$

where $q = M_2/M_1$ is the mass ratio, and where α, β and δ are the fractions of mass lost from the donor in the form of a direct fast wind, mass ejected from the vicinity of the accretor and from a circumbinary coplanar toroid (with radius, $a_r = \gamma^2 a$), respectively – see van den Heuvel (1994) and Soberman, Phinney & van den Heuvel (1997). The accretion efficiency of the accreting star is thus given by: $\epsilon = 1 - \alpha - \beta - \delta$, or equivalently:

$$\partial M_1 = -(1 - \alpha - \beta - \delta)\,\partial M_2 \tag{8}$$

where $\partial M_2 < 0$ (M_2 refers to the donor star). These factors will be functions of time as the binary system evolves during the mass-transfer phase. The general solution for calculating the change in orbital separation during the X-ray phase is found by integration of the orbital angular momentum balance equation (Eq. 5):

$$\frac{a}{a_0} = \Gamma_{ls}\left(\frac{q}{q_0}\right)^{2(\alpha+\gamma\delta-1)}\left(\frac{q+1}{q_0+1}\right)^{\frac{-\alpha-\beta+\delta}{1-\epsilon}} \times \left(\frac{\epsilon q+1}{\epsilon q_0+1}\right)^{3+2\,\frac{\alpha\epsilon^2+\beta+\gamma\delta(1-\epsilon)^2}{\epsilon(1-\epsilon)}} \tag{9}$$

where the subscript '0' denotes initial values and Γ_{ls} is factor of order unity to account for tidal spin-orbit couplings ($\dot{J}_{\rm ls}$).

In our standard model for the RLO we assumed a direct wind mass-loss fraction of $\alpha = 0.20$ and neglected the possibility of any circumbinary toroid (i.e. $\delta = 0$). Furthermore, we assumed the accretion rate onto the compact object to be limited by the Eddington luminosity and hence: $\beta \equiv max\left((|\dot{M}_{\rm donor}| - \dot{M}_{\rm Edd})/|\dot{M}_{\rm donor}|, 0\right)$, where $|\dot{M}_{\rm donor}|$ is the mass-transfer rate from the donor star. For a typical neutron star accreting hydrogen $\dot{M}_{\rm Edd} \simeq 1.5\times10^{-8}\,M_\odot\,{\rm yr}^{-1}$.

2.6 Gravitational waves and merging NS/BH binaries

In the Newtonian/quadrupole approximation ($a \ll \lambda_{\rm gwr}$) the merging timescale of a compact binary with semi-major axis, a and eccentricity, e is given by Peters (1964):

$$\tau_{\rm gwr}(a_0, e_0) = \frac{12}{19}\,\frac{C_0^4}{\beta} \times \int_0^{e_0} \frac{e^{29/19}[1 + (121/304)e^2]^{1181/2299}}{(1-e^2)^{3/2}}\,de \tag{10}$$

where

$$C_0 = \frac{a(1-e^2)}{e^{12/19}}\,[1 + (121/304)e^2]^{-870/2299} \tag{11}$$

can be found from the initial values (a_0, e_0), and the constant β is given by:

$$\beta = \frac{64G^3}{5c^5}M^2\mu \tag{12}$$

Here M and μ denote the total mass and the reduced mass of the system, respectively. The integral given above must be evaluated numerically. However, for circular orbits the merging timescale can easily be found analytically: $\tau_{\rm gwr}^{\rm circ} = a_0^4/4\beta$. The timescale is very dependent on both a and e. Tight and/or eccentric orbits spiral-in much faster than wider and more circular orbits – see Fig. 10. For example, we find that the double neutron star system PSR 1913+16 ($P_{\rm orb} = 7.75$ hr, $M_{\rm NS} = 1.441$ and $1.387\,M_\odot$, respectively) with an eccentricity of 0.617 will merge in 302 Myr; if its orbit was circular the merger time would be five times longer: 1.65 Gyr!

3 STAR FORMATION RATES, GALACTIC MODELS AND STARFORMING REGIONS

We have assumed that the star formation rate has been continuous in the Galactic disk as inferred from observations (e.g. Gilmore 2001). Furthermore, following Hurley, Tout & Pols (2002) we assume that one binary ($M_1 > 0.8\,M_\odot$) is born in the Galaxy per year. Hence, for the formation rate of a massive binary with primary star mass $> 10\,M_\odot$ and secondary star mass $> 4\,M_\odot$ we simply use:

$$\Phi_{\rm BSFR} = f\,0.01 \quad {\rm yr}^{-1} \tag{13}$$

where f is a factor $\sim$1 to scale all our derived formation and merger rates. We fix this rate over the lifetime of the Galaxy ($\sim$ 12 Gyr). This prescription should facilitate comparison with other studies.

3.1 Galactic potentials

We have evolved our binaries in the potential of spiral galaxies. The adopted potential is a model for the Milky Way made by Flynn, Sommer-Larsen & Christensen (1996) with a few corrections to the parameters (Sommer-Larsen, private communication 2002). The potential $\Phi(R,z)$ is modelled in cylindrical coordinates: R being the distance in the plane from the center of the galaxy, and z being the height above the plane. The potential is a sum of a dark matter halo Φ_H, a central component Φ_C and a disk Φ_D. The dark matter halo is assumed to be spherically symmetric:

$$\Phi_H = \frac{1}{2}V_H^2\ln(r^2 + r_0^2) \tag{14}$$

where $r^2 = R^2 + z^2$. The central part of the potential is made-up of two spherical components:

$$\Phi_C = -\frac{GM_{C_1}}{\sqrt{r^2 + r_{C_1}^2}} - \frac{GM_{C_2}}{\sqrt{r^2 + r_{C_2}^2}} \tag{15}$$

Table 2. Adopted parameters for the Galactic potential

Component	Parameter	Value
	r_0	8.5 kpc
	V_H	210 km s^{-1}
Bulge/Stellar halo	r_{C_1}	2.7 kpc
	M_{C_1}	$3.0\times10^9\ M_\odot$
Central Component	r_{C_2}	0.42 kpc
	M_{C_2}	$1.6\times10^{10}\ M_\odot$
Disk	b	0.3 kpc
	M_{D_1}	$6.6\times10^{10}\ M_\odot$
	a_1	5.81 kpc
	M_{D_2}	$-2.9\times10^{10}\ M_\odot$
	a_2	17.43 kpc
	M_{D_3}	$3.3\times10^9\ M_\odot$
	a_3	34.86 kpc

Here G is the gravitational constant, M_{C_1} and r_{C_1} are the mass and the core radius of the bulge/stellar halo term, while M_{C_2} and r_{C_2} are the mass and core radius of the inner core. The disk potential is modelled using a combination of three Miyamoto-Nagai potentials, see Miyamoto & Nagai (1975):

$$\Phi_{D_n} = \frac{-GM_{D_n}}{\sqrt{(R^2 + [a_n + \sqrt{z^2 + b^2}]^2)}}, \quad n = 1, 2, 3 \tag{16}$$

The parameters b and a_n are related respectively to the scaleheight and scalelength of the disk, and M_{D_n} are the masses of the three disk components. The parameter values for the Milky Way are found in Table 2.

To obtain potentials for galaxies with other masses than the Milky Way, we have scaled the parameters with the square root of the galaxy mass (assuming that the ratio of the components of the galaxies remains constant). This gives a constant surface brightness as observed, see e.g. Binney & Tremaine (1994).

Star formation takes place in two very distinct physical environments. Mostly in the extended disks of spiral and irregular galaxies, but also a significant fraction in the compact dense gas disks in the centers of galaxies. The central star formation happens in starbursts with very high star formation rates for 0.1–1.0 Gyr (Kennicut 1998), while star formation in the extended disk is steady or slowly exponentially decreasing (Bruzual & Charlot 1993). We have assumed that the distribution of birth places follow the density distribution of the extended disk. The latter can be found by applying Poisson's equation to the disk potential:

$$\nabla^2\Phi_D = 4\pi G\rho_D \tag{17}$$

Finally, we assume that the binaries are born with a velocity equal to the local rotational velocity.

4 RESULTS

The results presented in this paper are based on a typical simulation of 20 million ZAMS binaries with standard parameters as given in Table 3. Of these systems 99.9 % did not make it to the final stage. Most of these systems either merged during the CE and spiral-in phase or were disrupted by a supernova explosion.

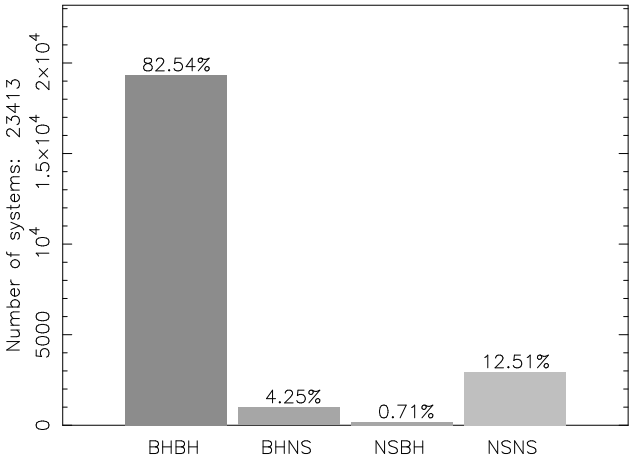

Figure 6. Relative formation ratios of binaries with neutron stars and/or black holes which will coalesce within 10 Gyr.

4.1 Relative formation ratios and merging timescales

The aim of this paper is to focus on GRB progenitors and burst sources of gravitational wave radiation. Therefore, we start out by showing in Fig. 6 the relative formation ratios of BHBH, BHNS, NSBH and NSNS systems which will merge within 10 Gyr. A total of 23 413 such sources is formed over a time interval of ∼2 Gyr from 20 million massive ZAMS binaries (see Table 3 for input parameters). It is seen that double black hole systems (BHBH) dominate this population and that only few close-orbit NSBH systems are formed. However, from Fig. 7 it is seen that the relative formation ratios of mergers do not represent the overall relative formation ratios of all massive double degenerate systems. Many NSBH, BHNS and BHBH systems are formed in very wide orbit systems ($P_{\rm orb} \gtrsim 100 - 1000$ yr) which will never merge ($\tau_{\rm merge} \sim 10^{21}$ yr). For these three categories the formation of such wide-orbit systems is even seen to be dominating. Almost all of the binaries formed in this right-hand peak of the bimodal $\tau_{\rm merge}$ distribution are caused by binaries which did not experience RLO from their secondary star (causing the orbits to widen subsequently from stellar wind mass loss and the effects of the second SN explosion). The majority of the wide-orbit BHNS systems also evolved without primary star RLO and thus remained detached binaries during their entire evolution. The same condition applies to $\sim 1/3$ of the wide-orbit BHBH systems, but none of the NSBH systems. The reason for the latter is that without RLO the secondary star will never end up with a mass above the threshold limit for making a black hole. Another interesting feature is that almost half of all the BHNS systems which merge within 10 Gyr evolve without primary star RLO. However, in these systems the black hole is shot into a closer orbit (due to the kick) which later, as a result of nuclear expansion, causes the secondary star to fill its Roche-lobe. This gives rise to the formation of a common envelope and spiral-in phase leading to a close final orbit. The same scenario is also responsible for ~ 5 % of the close-orbit NSNS systems. This formation channel (direct-supernova) of close-orbit systems was first discussed by Kalogera (1998) in the context of LMXBs. Another comment to Fig. 7 is that the population of close-orbit NSBH systems is clearly seen to be subdivided into two distinct populations. The systems with $\tau_{\rm merge} < 9$ Gyr evolved through helium star RLO (case BB) onto the NS whereas the systems with

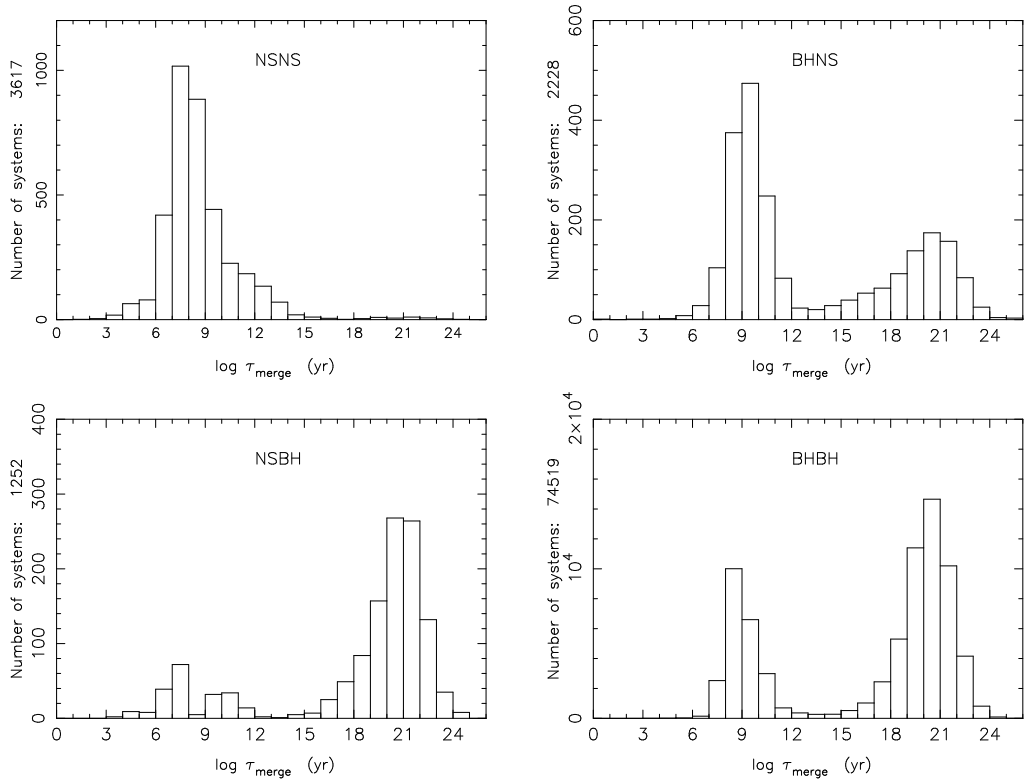

Figure 7. Histograms of merging timescales for binaries with neutron stars and/or black holes. The populations of NSBH, BHNS and BHBH are seen to be bimodal with a large component of very wide binaries with $\tau_{\rm merge} \sim 10^{21}$ yr. See text for a detailed discussion.

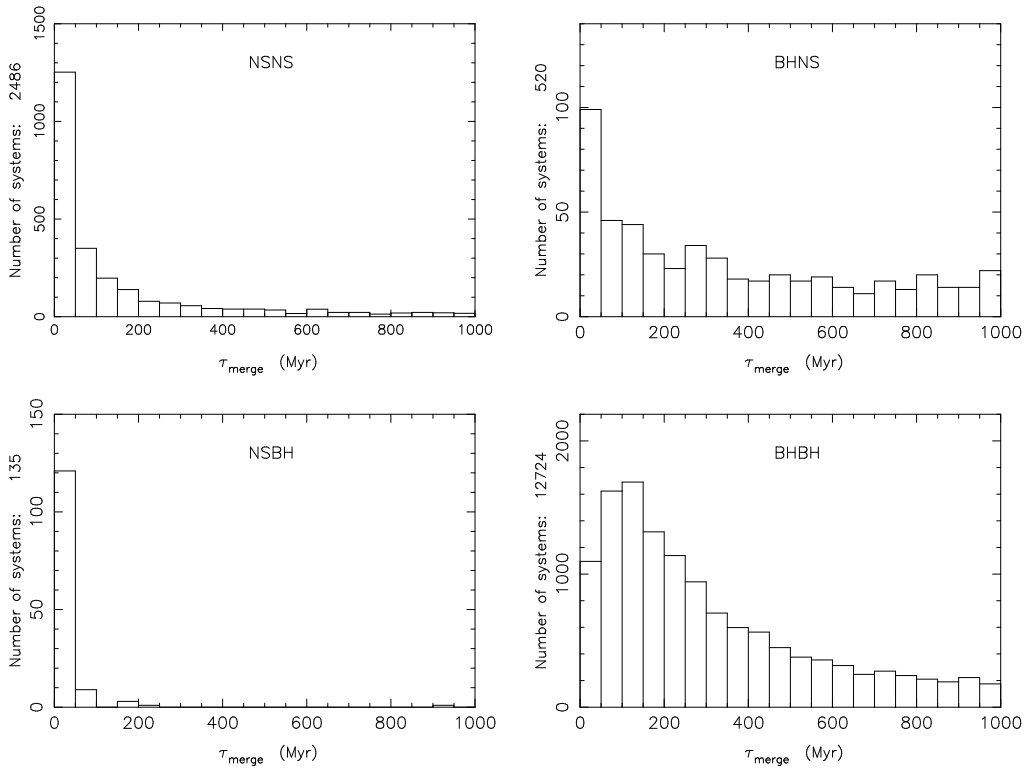

Figure 8. Histograms of merging timescales for binaries with neutron stars and/or black holes which coalesce within 1 Gyr.

Table 3. Adopted standard parameters for our binary population synthesis code. A typical simulation is based on 20 million ZAMS binaries.

Parameter	Symbol	Value	Note
Mass of primary star	$M_{\rm p}$	$10 - 100\,M_\odot$	Salpeter IMF (-2.7)
Mass of secondary star	$M_{\rm s}$	$4 - M_p$	the distribution is drawn to match the q-distribution
Initial ZAMS separation	a_0	$5 - 10\,000\,R_\odot$	a flat distribution in $\log a$
Stellar wind mass loss	α	0.20	
Timescale for RLO	$\Delta t_{\rm rlo}$	$\sim 3\,\tau_{\rm thermal}$	generally a good estimate
Critical mass ratio for CE	$q_{\rm ce}$	2.5	for a hydrogen donor star (at onset of RLO *after* wind mass loss)
Timescale for CE	$\Delta t_{\rm ce}$	1000 yr	upper limit
Efficiency of CE	$\eta_{\rm ce}$	0.5	+ liberated $E_{\rm acc}$, see Eq. 3
λ for CE	λ	$0.006 \sim 0.4$	individually calculated from stellar structure calculations, see Sec. 2.4
Core boundary parameter	$f_\lambda = \lambda^*/\lambda$	2	since $X \simeq 0.10$ may often underestimate the core mass (Tauris & Dewi 2001)
Critical He-star mass for CE	$M_{\rm He}^{\rm crit}$	$3.3\,M_\odot$	from recent helium donor star calculations (Dewi & Pols 2003)
λ for He-star CE	$\lambda_{\rm He}$	0.1	typical value from (Dewi & Pols 2003)
Maximum accretion rate	$\dot{M}_{\rm max}$	$\dot{M}_{\rm Edd}$	an Eddington accretion limit is applied to both NS and BH
kick-distribution for NS	w	$0 - 2000$ km s^{-1}	3 comp. Maxwellian [σ=30 (5%), 175 (80%) and 700 km s^{-1} (15%), respectively]
kick-distribution for BH	$w_{\rm bh}$	$0 - 2000$ km s^{-1}	same as above, but scaled: $w_{\rm bh} = w\,(M_{\rm ns}/M_{\rm bh})$ to yield same linear momentum

Table 4. The formation rates, the merger rates and the present population of massive double degenerate binaries in the Galactic disk – see text.

Systems	Formation rate	Merger rate	$N_{\rm Gal}$
NSNS	1.8×10^{-6} yr^{-1}	1.5×10^{-6} yr^{-1}	3 700
NSBH	6.3×10^{-7} yr^{-1}	8.4×10^{-8} yr^{-1}	6 400
BHNS	1.1×10^{-6} yr^{-1}	5.0×10^{-7} yr^{-1}	6 900
BHBH	3.7×10^{-5} yr^{-1}	9.7×10^{-6} yr^{-1}	320 000

$9 < \tau_{\rm merge}/{\rm Gyr} < 12$ evolved without helium star mass-transfer. A close-up of the distribution of merging timescales < 1 Gyr is presented in Fig. 8. The various populations have rather different distributions of $\tau_{\rm merge}$ – ranging from extremely short (NSBH) to somewhat flat (BHNS).

4.2 Galactic formation rates, merger rates and the present population of massive double degenerate binaries

In Table 4 we list our best estimate for the Galactic formation rate, the merger rate and the present population of massive double degenerate binaries. The present population in the Galactic disk is a rough estimate based on the difference in formation rate and merger rate integrated over the age of the Milky Way (12 Gyr) and corrected for: I) the systems escaping the gravitational potential of our Galaxy ($< 10\,\%$) and II) the contribution from the current population of potential mergers recently formed. The formation rate of NSNS systems is larger than that of both NSBH and BHNS systems. However, as we noticed from Fig. 7, discussed in the previous section, these latter systems form a large fraction of very wide-orbit binaries which will never merge and therefore accumulate in numbers with the age of the Galaxy. This is also seen from their relatively small merger rates. It is thus expected that the Galaxy hosts a larger number of NSBH and BHNS systems compared to NSNS systems. The BHBH systems, however, are seen to dominate the overall Galactic population of massive compact binaries. We estimate a present population above 300 000 systems in the Milky Way. Although such systems cannot be detected observationally yet (since they do not emit electromagnetic radiation) we may hope to detect continuous gravitational waves from some of these systems in our backyard once LISA has been launched.

In order to understand the large formation rate of BHBH binaries, and the origin of the different massive compact binaries, it is usefull to look at Fig. 9. It is clearly seen that the initial parameter space for the stellar component masses favour the formation of BHBH binaries. The lines separating the different populations in the diagram can largely be understood from the threshold masses listed in Table 1. The dividing lines are "fuzzy" since the initial orbital separation is also a determining factor for the outcome of the binary stellar evolution (i.e. a helium star's mass depends on at what evolutionary stage its progenitor star lost its hydrogen envelope). The lower curved line in the plot marks the onset of common envelope evolution. The line is curved (rather than straight) since the mass-ratio limit $q_{\rm ce}$ is evaluated *after* the wind mass loss is accounted for, prior to the RLO, and more massive stars loose a relatively larger fraction of their mass in the form of a stellar wind (see Fig. 2). We notice that no BHBH systems are formed which evolved through a CE-phase during the mass transfer from the primary star. The reason for this is the small values of the λ-parameter obtained from real stellar structure models. This reflects that the envelopes of these massive stars are tightly bound to their cores so that the binaries do not have enough orbital energy to expel the envelopes in the spiral-in phase. Therefore the systems will merge (and perhaps form Thorne-Żytkow objects).

4.3 Galactic double neutron star (NSNS) binaries

Simulating the formation of double neutron star binaries is a crucial test for the computer code and the physics assumptions being used. In Fig. 10 we have plotted the distribution of NSNS binaries at birth in a (separation, eccentricity)-diagram. We have partly used the location of the four known Galactic NSNS systems in the disk (see Table 5) to constrain our input parameters so we can reproduce these observed systems from simulations. Especially PSR J1518+4904 (Nice, Sayer & Taylor 1996) is a challenge for any binary population synthesis code given its low eccentricity (0.27) and relatively wide orbit $P_{\rm orb} = 8.6$ days ($a \simeq 25\,R_\odot$). We find that our simulated population fits the observations well given that the majority of the simulated NSNS systems merge on a timescale much shorter than the lifetime of the observed (recycled) pulsars. Furthermore, NSNS systems with $a \lesssim 1\,R_\odot$ ($P_{\rm orb} \lesssim$ 100 min.) are very difficult to detect as a result of the large acceleration of their pulsed signals. It is possible that this plot may help to

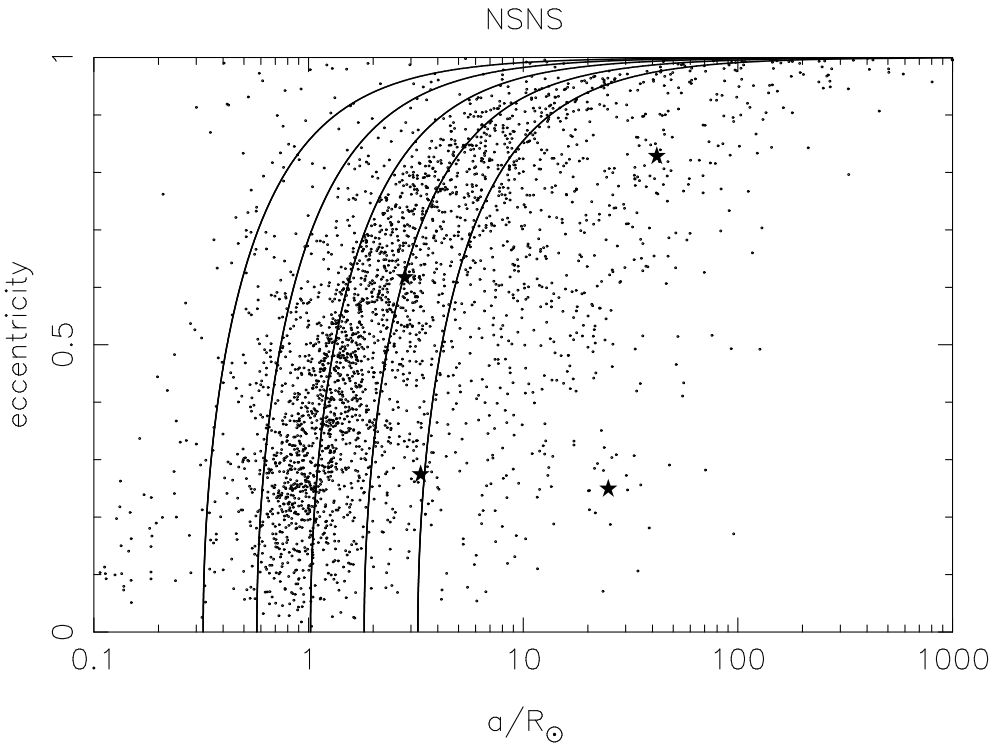

Figure 10. The simulated distribution of newborn double neutron star binaries in the (separation, eccentricity)-plane. Isochrones for the merging time of the double neutron star binaries are also shown. We calculated these assuming two $1.4\,M_\odot$ neutron stars in each binary. The curves correspond to values of: 3×10^5 yr, 3 Myr, 30 Myr, 300 Myr and 3 Gyr (from left to right), respectively. The four NSNS systems detected in the Galactic disk are indicated with stars.

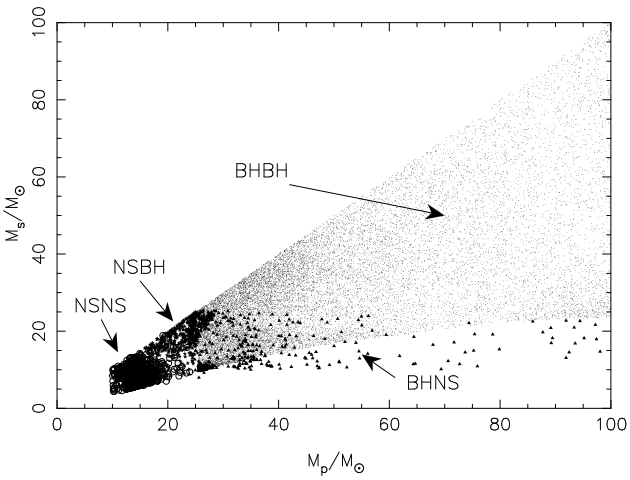

Figure 9. Initial primary and secondary stellar masses for 20 000 ZAMS binaries evolving all the way to form massive double degenerate systems.

converge some of the many various input parameters used in population synthesis codes today.

It is instructive to look at the distribution of kicks imparted to neutron stars in surviving binaries which evolved all the way to the final NSNS stage. This is shown in Fig. 11. The difference between the kicks imparted during the first and the second SN explosion is very significant: the average values of the selected kicks are $\bar{w}_1 = 53$ km s^{-1} and $\bar{w}_2 = 263$ km s^{-1}, respectively. In order

Table 5. The four observed double neutron star systems in the Galactic disk (for references see Nice, Sayer & Taylor 1996 and Lyne et al. 2000).

PSR-name	sep. $R_\odot$	ecc.	$M = M_1 + M_2$ $M_\odot$	$\tau \equiv P/2\dot{P}$ Myr
J 1518+4904	24.9	0.249	2.69	20 000
B 1534+12	3.33	0.274	2.68	200
J 1811–1736	41.9	0.828	2.6	900
B 1913+16	2.81	0.617	2.83	100
B 2127+11C*	2.86	0.681	2.71	100

* This system resides inside a globular cluster and has a different origin.

for the systems to avoid merging in the CE and spiral-in phase of the evolved secondary stars, the systems must be in a fairly wide orbit prior to the HMXB and subsequent CE and spiral-in phase. This means that these systems can only survive very small kicks in the first SN explosion in order to avoid disruption. On the other hand, after the CE and spiral-in phase the orbits of the surviving systems will always be tight and therefore the systems will be able to withstand even very large kicks in the second SN explosion. Actually, the distribution of selected kicks during the second SN resembles the input trial distribution of kicks plotted in Fig. 4. The corresponding systemic recoil velocities after the SNe were $\bar{v}_1 = 8.6$ km s^{-1} and $\bar{v}_2 = 220$ km s^{-1}, respectively. Thus, when considering the runaway properties of NSNS systems it is sufficient to consider the effects from the second SN.

To get an idea of the distance travelled by NSNS binaries from their birth place prior to their coalescence, one simply has to mul-

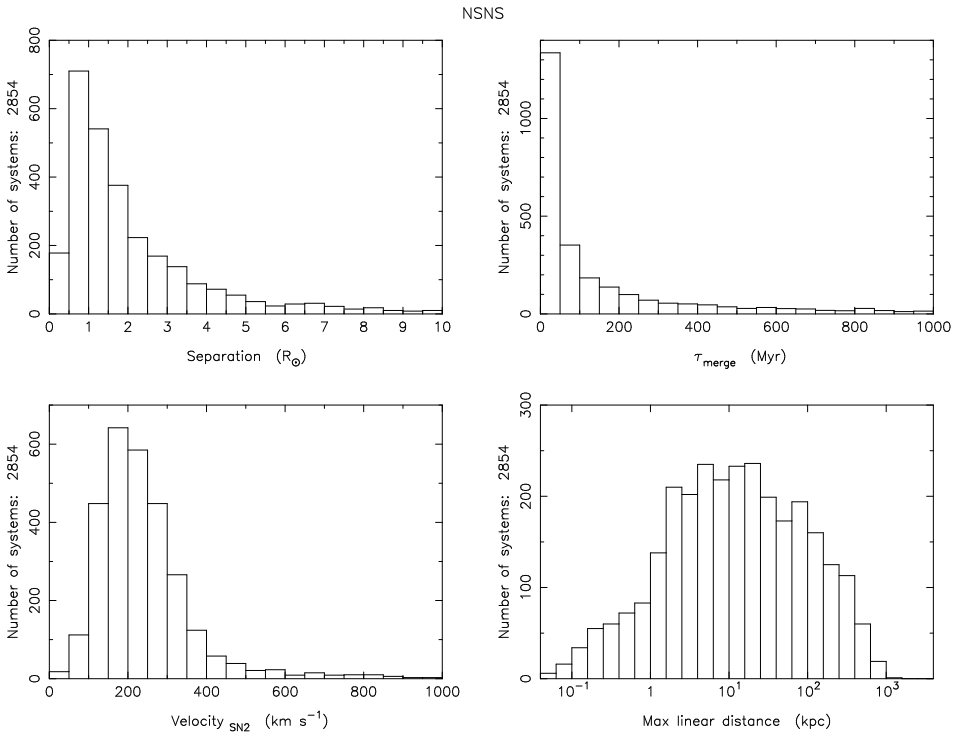

Figure 12. Distribution of newborn double neutron star binaries with respect to orbital separation, merging timescale, systemic (recoil) velocity from the second SN explosion and the maximum distance from the origin of birth in a host galaxy – see text for details.

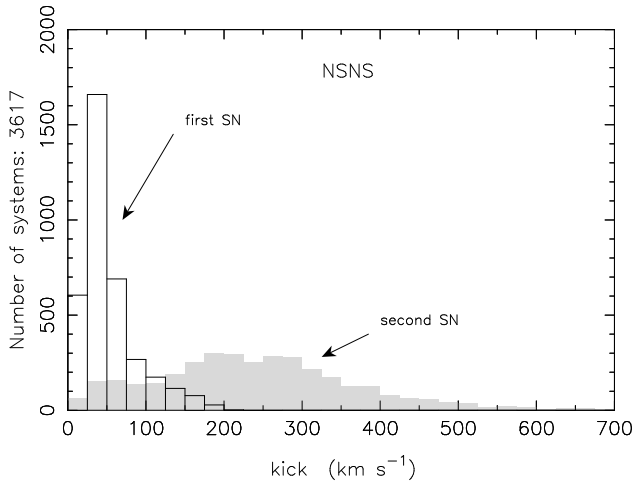

Figure 11. The distribution of kicks imparted to newborn neutron stars in *surviving* binaries. The difference in selected kicks between the first and second SN are expected from a binary evolutionary point of view – see text.

tiply their space velocity with the merging timescale. The space velocity is caused by the recoil of shell ejection combined with the asymmetric kick given to the neutron star at birth. In Fig. 12 we have plotted histograms of final orbital separation, merger time, space velocity and the estimated distance travelled before the merging event. In order for other readers to compare with our results we have in this plot simplified both the space velocity and the distance travelled. For the space velocity shown here it is assumed that the binary was at rest prior to the second SN (which is a good approximation, see above). The other approximation applied here is that the binary motion was without influence from the Galactic potential (this approximation gets exceedingly worse with increasing merger times). Hence, the estimated distance is an upper limit. We see that typical systems travel ∼10 kpc prior to their merging and that the distribution of distances travelled is rather broad. It should be mentioned that in our simulations presented throughout this paper the space velocities resulting from both SNe are added as vectors and the binary is moving in a Galactic potential as described in Section 3.

4.4 Offset distribution of mergers from their host galaxies

Recent work by Bloom, Kulkarni & Djorgovski (2002) shows that the median projected angular offset of 20 long-duration GRBs is only ∼1.3 kpc (0.″17 for an assumed cosmology of $\Omega_\Lambda = 0.7, \Omega_M = 0.3$ and $H_0 = 65$ km s^{-1} Mpc^{-1}). In Fig. 13 we have plotted our cumulative distribution of calculated projected radial distances in various host galaxies. For a random orientation of the radial distance with respect to the line-of-sight one finds the average projected radial distance (in the plane of the sky) by multiplying with a factor $\pi/4$. The panels in the left column show the result of launching our binaries into four galaxies with different masses (0.001–1 times the mass of the Milky Way). We see that roughly half of all massive compact binaries merge within a projected radial distance of 4 kpc for a 0.1 $M_{\rm MW}$ galaxy. Hence, the majority of these systems merge *inside* their host galaxies. However, the median distance is larger than the median value observed for the long-duration bursts. At a projected radial offset of 1.3 kpc we find that less than 25% of all BHNS, NSBH and NSNS systems merge (independent of

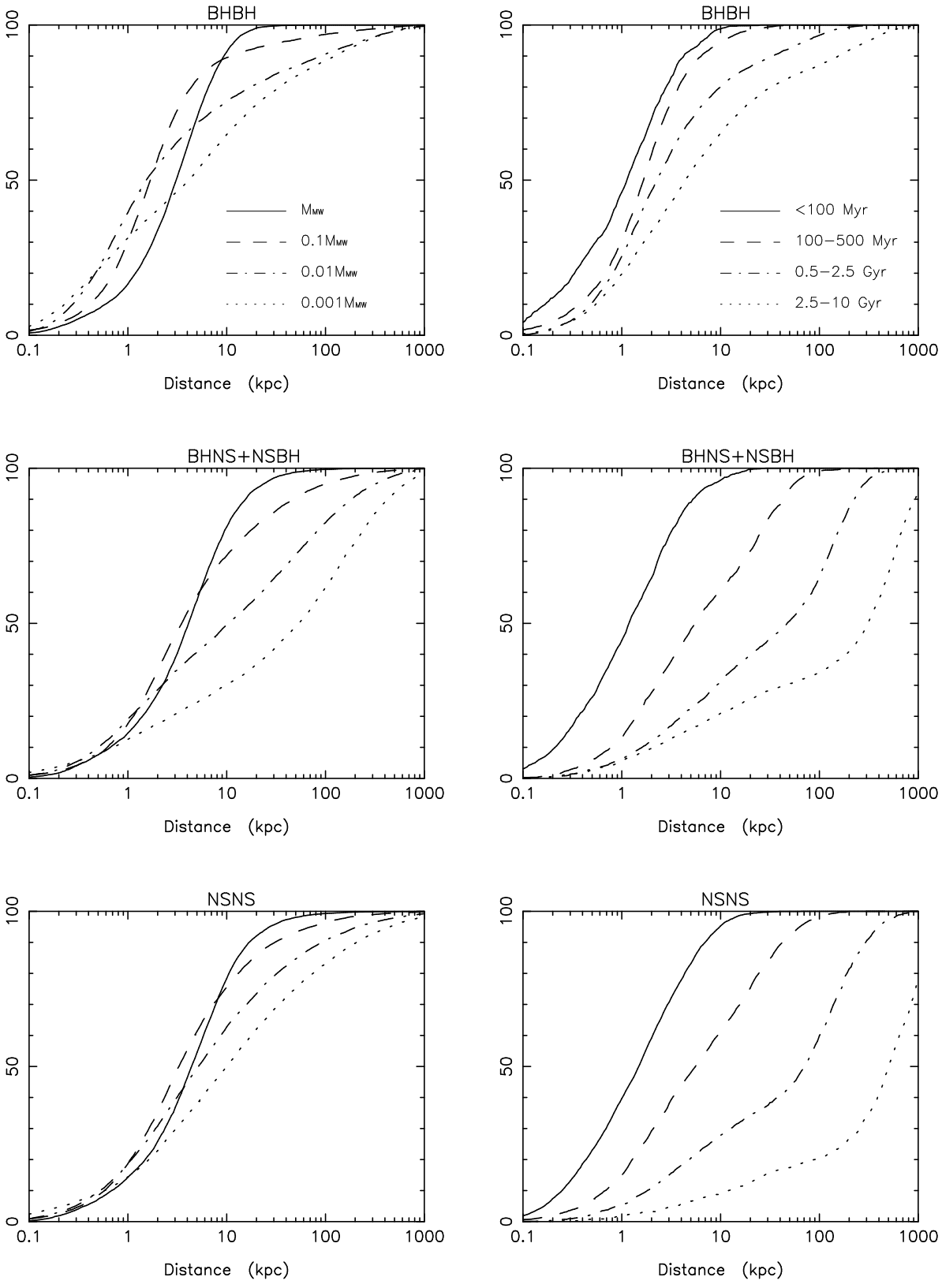

Figure 13. The panels in the left column shows the cumulative distribution of systems merging within the projected radial galactic distance given on the x-axis. Only binaries merging within 10 Gyr are included. We launched our binaries into four galaxies with different masses (0.001–1 times the mass of the Milky Way). The panels on the right-hand side are for a 0.1 $M_{\rm MW}$ galaxy. The curves represent four different merging timescale intervals – see text.

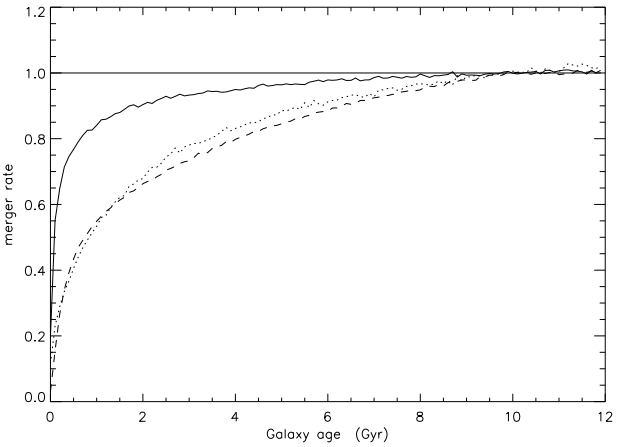

Figure 14. Merger rates (relative to present merger rates) as a function of the age of our Galaxy for NSNS systems (solid line), BHNS+NSBH systems (dashed line) and BHBH systems (dotted line) for a constant Galactic star formation rate. The curves show the emergence of a "steady state".

the mass of the host galaxy). In general, it therefore seems clear that merging compact objects most likely cannot be the progenitors of long-duration GRBs (as also concluded by Bloom, Kulkarni & Djorgovski 2002). However, from a pure kinematical point of view one cannot rule out that some of the long GRBs with afterglows could be associated with merging compact objects. It is also an interesting question to what extent such a merging event outside a galaxy would produce an afterglow at all. It should be noticed that the merging BHBH systems are only shown for comparison – they cannot be progenitors of GRBs. Note, that the central panel shows the mixed population of both NSBH and BHNS systems. The panels on in the right-hand side of the figure simply show how the cumulative fraction of systems merging increases as a function of projected radial galactic distance for a 0.1 $M_{\rm MW}$ galaxy. The curves represent four different merging timescale intervals: 0–100 Myr, 100–500 Myr, 0.5–2.5 Gyr and 2.5–10 Gyr, respectively. We find that ∼10 % of all NSNS systems formed escape our Galaxy.

Fig. 14 shows the merger rates of NSNS systems (solid line), BHNS+NSBH systems (dashed line) and BHBH systems (dotted line) for a constant Galactic star formation rate. Each of the merger rates are scaled relative to its present merger rate. In calculating this rate, only binaries merging within the age of the Milky Way are included. It is seen that the Milky Way today is in a "steady state" (i.e. the formation rate of systems in close orbits merging within 10 Gyr is equal to the number of systems merging per unit time).

4.5 Prospects for LIGO/VIRGO detection rates

LIGO I and LIGO II are expected to detect NSNS inspiral events out to a distance of ∼ 20 Mpc and ∼ 300 Mpc, respectively, according to recent estimates (Thorne 2001). This corresponds to wave amplitudes of roughly $10^{-20} > h > 10^{-22}$. As a result of the much larger chirp mass ($M_{\rm chirp} \equiv \mu^{3/5} M^{2/5}$) of the BHBH mergers, such binaries will be detected out to a distance luminosity, $d_L \propto M_{\rm chirp}^{5/6}$ (Finn 1998) which is about 4 times larger in average according to our estimates. Hence, the ratio of detected event rates for BHBH mergers relative to NSNS mergers is $4^3 \sim 64$ times larger than the corresponding ratio of such mergers in our Galaxy. Thus BHBH mergers will be completely dominant for LIGO detections (as noted by Sipior & Sigurdsson 2002). The exact value of the chirp mass ratio depends mainly on the black hole masses estimated at birth as well as the possibility of hypercritical accretion onto neutron stars. BHNS and NSBH mergers have a chirp mass which is roughy 2 times larger than that of the NSNS systems and thus the corresponding detected ratio of such mergers, relative to NSNS mergers, is ∼5 times larger than the Galactic ratio.

Table 6. The expected LIGO/VIRGO detection rates of compact mergers.

Systems	Galactic merger rate	LIGO I	LIGO II
NSNS	1.5×10^{-6} yr^{-1}	6.0×10^{-4} yr^{-1}	2.0 yr^{-1}
NSBH	8.4×10^{-8} yr^{-1}	1.7×10^{-4} yr^{-1}	0.6 yr^{-1}
BHNS	5.0×10^{-7} yr^{-1}	1.0×10^{-3} yr^{-1}	3.4 yr^{-1}
BHBH	9.7×10^{-6} yr^{-1}	2.5×10^{-1} yr^{-1}	840 yr^{-1}

In order to extrapolate the Galactic coalescence rate out to the volume of the universe accessible to LIGO, one can either use a method based on star formation rates, galaxy number density or a scaling based on the B-band luminosities of galaxies. Using the latter method Kalogera et al. (2001) found a scaling factor of $(1.0 - 1.5) \times 10^{-2}$ Mpc^{-3}, or equivalently, ∼ 400 for LIGO I (out to 20 Mpc for NSNS mergers). Since LIGO II is expected to look out to a distance of 300 Mpc (NSNS mergers), the volume covered by LIGO II is larger by a factor of $(300/20)^3$ and thus the scaling factor in this case, relative to the coalescence rates in the Milky Way, is about 1.3×10^6. Therefore, the expected rate of detections from galactic field NSNS inspiral events is roughly 2 yr^{-1} for LIGO II (see Table 6) and an impressive 840 yr^{-1} for the BHBH mergers! Even LIGO I may, with a bit of luck, detect an event from a BHBH collision. Beware, that our estimated merger rates should be considered as lower limits given that compact mergers in globular clusters probably also contribute significantly to the total merger rates (Portegies Zwart & McMillan 2000). The cosmological implications of gravitational wave observations of binary inspiral are also interesting to note (e.g. Schutz 1986; Finn 1997).

5 DISCUSSION

5.1 The dependence on input parameters

Monte Carlo simulations is a powerful tool for investigating complicated interactions which depend on many parameters. Often the difficult task is not to produce a reasonable code but to analyse the results, pinpoint the important physical parameters behind the major trends in a simulated population and try to understand these results in terms of relatively simple physics.

In Table 7 we summarize the effects of various input parameters on the formation and evolution of massive double degenerate systems. Model A is our standard model. In all other models we modified one parameter at a time, keeping all the other parameters as in our standard model. Model B having a constant $\lambda = 0.5$ is a very bad approximation (see Fig. 5), but nevertheless it is apparently still used in many computer codes. For example it is clear that the formation channel recently presented in Fig. 1 of Belczynski, Bulik & Kalogera (2002) will not work if one applies a reasonable realistic value for the binding energy of the envelope. At stage V in their figure, one can use a stellar structure model

Table 7. Galactic relative formation ratios, formation rates and merger rates of massive compact binaries. Model A is our best estimate. See text.

Model/ Systems	Rel. formation %	Formation rate Myr^{-1}	Merger rate Myr^{-1}
A) standard			
NSNS	4.4	1.8	1.5
NSBH	1.5	0.63	0.08
BHNS	2.7	1.1	0.50
BHBH	91.3	37	9.7
B) $\lambda = 0.5$ constant			
NSNS	7.6	20	17
NSBH	2.3	6.1	3.7
BHNS	1.9	4.9	1.3
BHBH	88.2	230	76
C) kick: $0.5\,\sigma_w$			
NSNS	6.5	7.2	3.3
NSBH	3.6	4.0	0.34
BHNS	3.4	3.8	1.3
BHBH	86.5	96	18
D) core: $f_\lambda = 1$			
NSNS	3.6	1.1	0.95
NSBH	1.6	0.48	0.04
BHNS	2.9	0.61	0.16
BHBH	92.7	27	1.3
E) IMF: $f \propto M_p^{-2.0}$			
NSNS	4.4	1.9	1.4
NSBH	1.6	0.66	0.08
BHNS	2.9	1.2	0.54
BHBH	91.0	37	9.8
F) wind: $\alpha = 0$			
NSNS	2.8	1.1	0.83
NSBH	3.5	1.4	0.22
BHNS	2.0	0.77	0.22
BHBH	91.8	36	7.2
G) $q_{\mathrm{ce}} = 2.0$			
NSNS	3.6	1.3	1.0
NSBH	1.5	0.54	0.08
BHNS	3.7	1.3	0.44
BHBH	91.2	32	6.9
H) $q_{\mathrm{ce}} = 3.0$			
NSNS	5.2	2.4	1.9
NSBH	1.5	0.71	0.11
BHNS	3.7	1.7	1.1
BHBH	89.5	41	12
I) $q_{\mathrm{ce,He}} = 2.5$			
NSNS	2.3	0.93	0.54
NSBH	1.5	0.62	0.02
BHNS	2.9	1.2	0.57
BHBH	93.3	38	9.7
J) $\Delta E_{\mathrm{acc}} = 0$			
NSNS	4.2	1.4	1.3
NSBH	2.2	0.71	0.06
BHNS	2.2	0.71	0.21
BHBH	91.4	30	3.4
average (D→J)			
NSNS	3.7	1.5	1.1
NSBH	1.9	0.74	0.09
BHNS	2.9	1.0	0.47
BHBH	91.6	34	7.2

and estimate a value of $\lambda = 0.23$ for the $R = 82\,R_\odot$ donor star of mass $14.1\,M_\odot$. This results in a post-CE separation which is roughly 3 times *smaller* than the radius of the descendant helium star. Hence, this system is doomed to coalesce (if one excludes the internal thermodynamic energy when estimating the value of λ the problem even exacerbates). Model C seems to give too small values of the kick velocity compared to observations of radio pulsars (Cordes & Chernoff 1998). At the bottom of the table the average result of models D–J is given. It is interesting to notice that these values are not very different from our standard model results.

5.2 The Galactic supernova rate

We have based the calibration of our models on the star formation rate for the Milky Way (see Eq. 13). In order to check the validity of this calibration we have compared our simulated Galactic supernova rate of type Ib/c SNe with the empirical estimates of Cappellaro et al. (1999). If we assume that all type Ib/c SNe originate from the collapse of naked stars which have lost their hydrogen/helium envelopes as a result of mass transfer in a binary system, then we find a rate of: $f\,0.28$ (100 yr)$^{-1}$. We can compare this result with a rate of 0.14 SNu (1 SNu = 1 SN (100 yr)$^{-1}$ ($10^{10}\,L_\odot^B$)$^{-1}$) given in Table 4 in Cappellaro et al. (1999). The B-band luminosity of the Milky Way is $\sim$ a few times $10^{10}\,L_\odot$ and therefore our calibration seems to be about right.

5.3 Comparison with other studies

The expected LIGO/VIRGO detection rates can be determined either from binary population synthesis calculations, or from observations of Galactic NSNS systems (binary pulsars). Both methods involve a large number of uncertainties – see the excellent review by Kalogera et al. (2001) and references therein. Current estimates for the Galactic merger rate of NSNS systems converge between 10^{-6} – 10^{-4} yr^{-1}. Our results belong to the lowest end of this interval. However, notice from Table 7 that if (*when*) other population synthesis codes start using real λ-values (rather than a constant) their merger rates will go down by a factor of $\sim$10.

In general there is no consensus on the formation ratios of the various compact binaries. This is due to the λ-values discussed in this paper, the helium star evolution and the unsettled question of hypercritical accretion. Studies including hypercritical accretion adopt different approaches and do not agree on the extend and outcome of this effect. Studies including this process turn many of the (first-born) neutron stars into black holes, resulting in a much larger ratio of BHNS/NSNS. In our study we find a relatively high number of BHBH systems being formed. We wonder if other codes reject systems which do not evolve through a (semi-detached) contact phase (i.e. if the primary star evolves to giant dimensions without filling its Roche-lobe). As we have seen in this study, the direct-supernova mechanism (Kalogera 1998) forms a significant fraction ($\sim$1/3) of all close-orbit BHNS systems and also contributes ($\sim$5%) somewhat to the formation of NSNS mergers.

The distribution of separations (or lifetimes) of the merging binaries is roughly in agreement with the results of other recent studies. The double neutron stars in the study of Belczynski, Kalogera & Bulik (2002) have slightly tighter orbits. This is mainly due to their higher limit of $M_{\mathrm{He}}^{\mathrm{crit}}$ resulting in more systems going through a second common envelope phase. Their BHNS systems are marginally wider than ours, since their progenitors all are more massive than this limit. The distribution of NSNS separations found

by Bloom, Sigurdsson & Pols (1999) is close to ours, even though they have not included mass transfer from a helium star. This is somewhat a surprise since it is required that the helium stars lose their envelope in order to form very tight orbits without merging.

We find our distribution of space velocities of the merging binaries to closely resemble both that of Belczynski, Kalogera & Bulik (2002), and that of Bloom, Sigurdsson & Pols (1999). Our distribution of merger sites mostly rely on the lifetimes and space velocities, and is therefore also in agreement with their studies.

Our parameter variation studies show that the distributions of lifetimes and space velocities of the merging binaries are quite stable (unlike the formation rates). This might seem somewhat surprising. If, as an example, the inspiral of the neutron star during the common envelope is more efficient, then it would seem that the distribution of NSNS systems should become tighter. This does not happen due to the fact that only a limited range of post-inspiral distances lead to survival of NSNS systems. If the orbit becomes too tight the neutron star merges with the core of the giant. If, on the other hand, the orbit is too wide then the supernova explosion is likely to disrupt the binary.

5.4 Progenitors of short-duration GRBs

As discussed in the introduction, it seems likely that one needs a disk of nuclear matter around a black hole in order to produce a GRB. Such a disk can be formed by the collapse of the core of a massive star or by a merger of either a double neutron star or a mixed neutron star/black hole system. The merger of a black hole and a white dwarf (Fryer et al. 1999), or the merger of a neutron star or black hole with a CO- or helium core (Fryer & Woosley 1998), as a result of spiral-in in a CE, may not be a good candidate for producing a short-duration GRB. One concern is that a white dwarf, or a CO/He-core, is a relatively low-density object compared to nuclear matter and it has a relatively large dimension (> 5000 km). The resultant disk would probably then be accreted much slower than needed for making a short-duration GRB. Merging double black holes are not candidates either due to the complete lack of any accretion disk. Therefore, we only considered the merging of double neutron stars (NSNS) or neutron star/black holes (BHNS and NSBH) as progenitors of the short-duration GRBs.

5.5 Do all GRBs origin from binaries ?

It is interesting to notice that most fireball models eject only a little matter ($\sim 10^{-5}\,M_\odot$) and require a rotating progenitor. To minimize the amount of ejected matter, collapsars require that the hydrogen envelope of the massive star has been removed before the collapse (MacFadyen & Woosley 1999). So the progenitors are in fact rotating helium stars (Wolf-Rayet stars) collapsing into black holes. Strong winds could remove the hydrogen envelope but may also remove too much spin angular momentum. An effective way of removing the envelope is via RLO in a binary system. Hence, it is possible that *all* GRBs origin from massive interacting binaries. In a recent paper (Lee, Brown & Wijers 2002) it has been suggested that indeed collapsars (hypernovae) are formed in tight binaries and that soft X-ray transients (SXTs) with black hole accretors are the *descendants* of GRBs.

5.6 Hypercritical accretion

It has been argued that a neutron star engulfed in a common envelope might experience hypercritical accretion and thereby collapse into a black hole (e.g. Chevalier 1993; Brown 1995). However, this idea seems difficult to conciliate with the observations of a number of very tight-orbit binary pulsars (Tauris, van den Heuvel & Savonije 2000). For example, the system PSR J1756–5322 which has a CO white dwarf companion ($\sim 0.7\,M_\odot$) with an orbital period of only 0.45 days. From an evolutionary point of view there is currently no other way to produce such a system besides from a CE and spiral-in phase. From a theoretical point of view it has been argued that the hypercritical accretion can be inhibited by rotation (Chevalier 1996) and strong outflows from the accretion disk (Armitage & Livio 2000). A number of other population synthesis studies have included hypercritical accretion as always leading to collapse of the neutron star (e.g. Fryer, Woosley & Hartmann 1999), or as an intermediate approach in which collapse only happens if the neutron star accretes a certain amount of matter (e.g. Belczynski, Bulik & Kalogera 2002). In the latter case a new parameter, the critical mass for a neutron star to collapse into a black hole is introduced (depending on the equation of state of neutron stars). Note however, that the masses of neutron stars determined in all of the five detected double neutron star systems are quite similar and close to a value of $1.4M_\odot$. Hence, in all these cases it is clear that the first-born neutron star did not accrete any significant amount of material from the common envelope. For the reasons mentioned above, we currently refrain from the possibiliby of hypercritical accretion onto neutron stars which successfully eject the envelope of their companion star.

6 CONCLUSIONS

We have performed binary population synthesis in order to estimate the properties of massive compact binaries. In particular we have focused on the kinematics of close-orbit binaries which merge within a Hubble-time as a result gravitational wave radiation. Our simulated populations of massive double degenerate systems are relatively stable against variation of the parameters of the code.

On a number of points we find that our description is more advanced than the work previously published in the literature:

- We have used realistic values of the λ-parameter of the common envelope and spiral-in evolution. We estimated this parameter for each individual binary donor star.
- We have used realistic models for the evolution of helium stars and included the effects of mass transfer from helium stars.
- We have included the effects of energy feedback from an accreting compact object in the common envelope evolution.
- We have applied reduced kicks to black holes in accordance with observations of black hole binaries.

We find that the formation rate and merger rate of massive double degenerate binaries is dominated by double black holes systems. The merger rates and the number of such systems present in our Galaxy today are estimated to be (based on model A):

- The Galactic merger rate of BHBH systems is $\sim 9.7\times10^{-6}$ yr^{-1} and the present disk population is $\sim 320\,000$ systems
- The Galactic merger rate of BHNS systems is $\sim 5.0\times10^{-7}$ yr^{-1} and the present disk population is $\sim 6\,900$ systems
- The Galactic merger rate of NSBH systems is $\sim 8.4\times10^{-8}$ yr^{-1} and the present disk population is $\sim 6\,400$ systems

- The Galactic merger rate of NSNS systems is $\sim 1.5\times10^{-6}$ yr^{-1} and the present disk population is $\sim$ 3 700 systems

The reason for the relatively low value of e.g. the NSNS merger rate is a result of our use of realistic λ-values. The mixed neutron star/black hole binaries have somewhat lower formation rates than the NSNS binaries, but a slightly larger population present in the Milky Way today, as a result of their longer merging timescales. Our studies also reveal an accumulating numerous population of very wide-orbit BHBH systems which never merge.

We estimate the detection rate for LIGO II and find that this rate is totally dominated (> 99 %) by BHBH mergers:

- $\sim$840 yr^{-1} for the BHBH mergers
- $\sim$3.4 yr^{-1} for the BHNS mergers
- $\sim$0.6 yr^{-1} for the NSBH mergers
- $\sim$2.0 yr^{-1} for the NSNS mergers

With a bit of luck LIGO I may detect a merging event of a BHBH system (0.25 yr^{-1}). The numbers quoted above are from model A. For other reasonable choices of parameter values these numbers typically differ within a factor of $\sim$2 (see Table 7).

We have also explored the movement of the binaries in the gravitational potential of galaxies. This allows us to estimate the distribution of merging offsets from the centers of the galaxies. We find that a large fraction of the compact binaries are retained within the massive galaxies, but for lower galaxy masses these binaries are able to escape and merge outside the galaxies. This result is not consistent with the observed offset distribution of long-duration GRB afterglows. We therefore conclude that merging compact objects cannot account for the ensemble of GRB offset distributions observed today – e.g. simulated NSNS binaries have a median projected radial (offset) distance of $\sim$ 4 kpc with respect to their host galaxy, while the observed value from 20 long-duration GRBs is only $\sim$ 1.3 kpc.

ACKNOWLEDGMENTS

We thank Onno Pols for providing helium star models. We also thank Jasinta Dewi and Ed van den Heuvel for discussions. T.M.T gratefully acknowledges support from the Danish Natural Science Research Council under grant no. 56916.

REFERENCES

Armitage P.J., Livio M., 2000, ApJ, 532, 540
Belczynski K., Bulik T., Kalogera V., 2002, ApJ, 571, L147
Belczynski K., Kalogera V., Bulik T., 2002, ApJ, 572, 407
Binney J., Tremaine S., 1994, Galactic Dynamics (Princeton University Press)
Blaauw A., 1961, Bull. Astr. Inst. Neth., 15, 265
Bloom J. S., et al., 1999, Nature, 401, 453
Bloom J. S., Sigurdsson S., Pols O. R., 1999, MNRAS, 305, 763
Bloom J. S., Kulkarni S. R., Djorgovski S. G., 2002, AJ 123, 1111
Brown G. E., 1995, ApJ, 440, 270
Brown G. E., Lee C. H., Bethe H. A., 1999, New Astronomy, 4, 313
Bruzual G.A., Charlot S., 1993, ApJ, 405, 538
Cappellaro E., Evans R., Turatto M., 1999, A&A, 351, 459
Chevalier R. A., 1993, ApJ, 411, L33
Chevalier R. A., 1996, ApJ, 459, 322
Cordes J. M., Chernoff D. F., 1998, ApJ, 505, 315
de Jager C., Nieuwenhuijzen H., van der Hucht K. A., 1988, A&AS, 72, 259
de Kool M., 1990, ApJ, 358, 189
Dewey R. J., Cordes J. M., 1987, ApJ, 321, 780
Dewi J. D. M., Pols O. R., 2003, MNRAS, submitted
Dewi J. D. M., Tauris T. M., 2000, A&A, 360, 1043
Dewi J. D. M., Tauris T. M., 2001, in Evolution of Binary and Multiple Star Systems, ed. P. Podsiadlowski et al., (ASP Conf. Vol. 229) p. 255
Dewi J. D. M., Pols O. R., Savonije G. J., van den Heuvel E. P. J., 2002, MNRAS, 331, 1027
Eichler D., Livio M., Piran T., Schramm D. N., 1989, Nature, 340, 126
Ergma E., van den Heuvel E. P. J., 1998, A&A, 331, L29
Finn L. S., 1997, in Gravitation & Cosmology, eds. S. Dhurandhar & T. Padmanabhan, (Klüwer, Netherlands) p. 95
Finn L.S., 1996, Phys. Rev. D53, 2878
Flynn C., Sommer-Larsen J., Christensen P., 1996, MNRAS, 281, 1027
Fruchter A. S., et al., 1999, ApJ, 516, 683
Fryer C. L., Woosley S. E., 1998, ApJ, 502, L9
Fryer C. L., Woosley S. E., Hartmann D. H., 1999, ApJ, 526, 152
Fryer C. L., Woosley S. E., Herant M., Davies M. B., 1999, ApJ, 520, 650
Fryer C. L., Heger A., 2000, ApJ, 541, 1033
Galama T. J., et al., 2000, ApJ, 536, 185
Gilmore, G., 2001, in Galaxy Disks and Disk Galaxies, ed. J.G. Funes & E.M. Corsini, (San Francisco, ASP)
Goodman J., 1986, ApJ, 308, L17
Habets G. M. H. J., 1986, A&A, 167, 61
Han Z., Podsiadlowski P., Eggleton P. P., 1994, MNRAS, 270, 121
Han Z., Podsiadlowski P., Eggleton P. P., 1995, MNRAS, 272, 800
Han Z., Podsiadlowski P., Maxted P. F. L., Marsh T. R., Ivanova N., 2002, MNRAS, 336, 449
Hurley K., et al., 1992, A&AS, 92, 401
Hurley J. R., Tout C. A., Pols O. R., 2002, MNRAS, 329, 897
Kalogera V., 1998, ApJ, 493, 368
Kalogera V., Narayan R., Spergel D. N., Taylor J. H., 2001, ApJ, 556, 340
Kennicut R. C. Jr., 1998, ARA&A, 36, 189
Kouveliotou C., Meegan C., Fishman G., et al, 1993, ApJ, 413, L101
Kuiper G. P, 1935, PASP, 47, 15
Kulkarni S. R., et al., 1998, Nature, 395, 663
Kulkarni S. R., et al., 1999, Nature, 398, 389
Lai D., Chernoff D. F., Cordes J. M., 2001, ApJ, 549, 1111
Landau L. D., Lifshitz E., 1958, The Classical Theory of Fields, (Pergamon Press, Oxford)
Lee H. K., Wijers R. A. M. J., Brown G. E., 2000, Phys. Rep., 325, 83
Lee C. H., Brown G. E., Wijers R. A. M. J., 2002, ApJ, 575, 996
Lee T., Petrosian V, 1997, ApJ, 474, 37
Lee W. H.., Kluzniak W., 1998, Gamma-Ray Bursts, 4th Huntsville Symposium, 798
Lyne A.G., Camilo F., Manchester R. N., et al., 2000, MNRAS, 312, 698
MacFadyen A., Woosley S. E., 1999, ApJ, 524, 262
Mazets E., et al., 1981, Ap&SS, 80, 119
Meszaros P., Rees M. J., 1992, ApJ, 397, 570
Meszaros P., Rees M. J., Wijers, R. A. M. J, 1999, New Astronomy, 4, 303
Metzger M. R, et al., 1997, Nature, 387, 878
Mirabel, et al., 2002, A&A, in press
Miyamoto M., Nagai R., 1975, PASJ, 27, 533
Nelemans G., Tauris T. M., van den Heuvel E. P. J., 1999, A&A, 352, L87
Nelemans G., van den Heuvel E. P. J., 2001, A&A, 376, 950
Nice D. J., Sayer R. W., Taylor J. H., 1996, ApJ, 466, L87
Nieuwenhuijzen H., de Jager C., 1990, A&A, 231, 134
Norris J., Scargle J., Bonnell J., 2000, BAAS, 32, 1244
Nugis T., Lamers H. J. G. L. M., 2000, A&A, 360, 227
Paczyński B., 1990, ApJ, 348, 485
Panaitescu A., Kumar P., Narayan R., 2001, ApJ, 561, L171
Perna R., Belczynski K., 2002, ApJ, 570, 252
Peters P. C., 1964, Phys.Rev, 136, B1224
Pfahl E., Rappaport S. A., Podsiadlowski P., 2002, ApJ, 573, 283
Piran T., 2000, Phys.Rep, 333, 529
Piro L., et al., 1999, ApJ, 514, L73
Piro L., et al., 2000, Science, 290, 955

Podsiadlowski P., Rappaport S. A., Han Z., 2002, MNRAS, submitted (astro-ph/0207153)
Pols O. R., Tout C. A., Eggleton P. P., Han Z., 1995, MNRAS, 274, 964
Pols O. R., Schröder K. P., Hurley J. R., Tout C. A., Eggleton P. P., 1998, MNRAS, 298, 525
Portegies Zwart S. F., McMillan S. L. W., 2000, ApJ, 528, L17
Portegies Zwart S. F., Yungelson L. R., 1998, A&A, 332, 173
Reichart D. E., 1999, ApJ, 521, L111
Ruffert M., Janka H. T., 1999, A&A, 344, 573
Sahu K. C., et al., 1997, Nature, 387, 476
Scalo J. M, 1986, Fundam. Cosmic Phys., 11, 1
Schaller G., Schaerer D., Meynet G., Maeder A., 1992, A&AS, 96, 269
Schutz B.F., 1986, Nature, 323, 310
Sipior M. S., Sigurdsson S., 2002, ApJ, 572, 962
Soberman G. E., Phinney E. S., van den Heuvel E. P. J., 1997, A&A, 327, 620
Taam R.E., Sandquist E.L., 2000, ARA&A 38, 113
Tauris T.M., 2001, in Evolution of Binary and Multiple Star Systems, ed.¶. Podsiadlowski et al., (ASP Conf. Vol. 229) p. 145
Tauris T. M., Dewi J. D. M., 2001, A&A, 369, 170
Tauris T. M., van den Heuvel E. P. J., Savonije G. J., 2000, ApJ, 530, L93
Tauris T. M., van den Heuvel E. P. J., 2003, in Compact Stellar X-ray Sources, ed. W. Lewin & M. van der Klis (Cambridge University Press)
Thorne K. S., 2001, LIGO Document Number P-000024-00-D
van den Heuvel E. P. J., 1994, in Interacting Binaries, Saas-Fee course 22, (Springer, Heidelberg) p. 263
Verbunt F., Phinney E.S., 1995, A&A, 296, 709
Vietri M., Perola C., Piro L., Stella L., 1999, MNRAS, 308, 29
Webbink R.F., 1984, ApJ, 277, 355
Wellstein S., Langer N., 1999, A&A, 350, 148
Woosley S.E., 1993, ApJ, 405, 273
Woosley S.E., Langer N., Waever T.A., 1995, ApJ, 448, 315
Yoshida A., et al., 1999, A&AS, 138, 433